# Metrological characteristics of a group of quadrupole partial pressure analyzers

L. Lieszkovszky, A. R. Filippelli, and C. R. Tilford
*National Institute of Standards and Technology, Gaithersburg, Maryland 20899*

(Received 16 January 1990; accepted 28 April 1990)

Linearity and stability of the pressure response of five different commercial quadrupole partial pressure analyzers and the influence of ion source parameters (emission current, electron energy, and ion energy) on the response has been investigated over the range $10^{-7}$–$10^{-1}$ Pa for He, $N_2$, and Ar. In the $10^{-3}$–$10^{-1}$ Pa range, each instrument developed a maximum (as large as a factor of 100 in one instrument) in the sensitivity versus pressure relation when operated with "low" ion energy (about 2–3 eV). All but one of the instruments also showed significant low-pressure nonlinearity, down to pressures as low as $10^{-7}$ Pa in one instrument, when operated at "high" ion energies (greater than about 7 eV). These results bring into question the often-assumed linearity of such instruments at low pressures. The dependence of the signal developed from a constant pressure ($10^{-6}$ Pa) trace gas as a function of the pressure of another gas (the matrix) was studied using He and Ar as the trace and matrix, and vice versa. The results demonstrated an apparent correlation between the magnitude of this dependence, and an instrument's nonlinearity as a function of pressure with the matrix gas alone. Brief exposures to certain active gases ($O_2$, $C_3H_8$, $CO_2$, CO) were found to cause shifts as large as 10% in the instruments' inert gas sensitivities (He, $N_2$, Ar). Tens of hours were required to return to pre-exposure sensitivities. Absolute argon sensitivity, monitored over a period of 220 days, for a standard set of operating parameters and with Faraday cup ion detection, showed initial one-directional changes as large as a factor of 2 for one instrument and a scatter of about $\pm$ 20% in all the instruments. The very large differences among the five test instruments with regard to sensitivity, linearity, and stability, as well as the influence of one gas on the sensitivity to another, point out the need for careful characterization and calibration of such instruments for all except the most qualitative applications.

## I. INTRODUCTION

For many vacuum applications, the partial pressures of certain component species of a gas are of more interest than the total pressure of the gas in a system. Partial pressure measurements are generally made with mass spectrometer-type instruments, commonly known as partial pressure analyzers (PPAs) or residual gas analyzers. Hereafter, these instruments will be referred to as PPAs. These instruments are generally smaller and less expensive than many analytical-type mass spectrometers, and are designed to be attached as an appendage instrument to an independent vacuum system. In many cases, particularly where PPAs are used to analyze the residual gases in a vacuum system, the absolute partial pressures are not so important; rather, the primary interest is in the relative partial pressures of molecular species (e.g., $H_2$ O, $N_2$, $O_2$, CO) that are indicative of the condition of the vacuum system. In other cases, such as process control or the measurement of absolute leak rates, it is necessary to determine the pressure of one or more gas constituents in absolute units, e.g., Pascals (1 millibar = 100 Pa, 1 Torr = 133.322 Pa). In any case, some level of calibration of the instrument is necessary in order to convert the instrument output (amps) to either relative or absolute pressure units.

The calibration may be performed by the manufacturer (i.e., the instrument as supplied, has a readout expressed in pressure units), the instrument may be calibrated by an independent calibration laboratory or by the user. In each case, as with all calibrations of any type of instrument, the question must be asked, "How accurate will the results be at the time of use?" This question may be particularly pertinent in the case of instruments with output in pressure units but no information from the manufacturer as to the uncertainty of the indicated partial pressures. In general, the accuracy of the results will depend on two factors. First is the calibration procedure, i.e., the accuracy of the reference standard and the adequacy of the calibration system. The second, and often more important factor is the performance of the instrument. Critical questions about PPA performance include: How stable is the instrument response with time? How dependent is the response on the history of use of the instrument? How linear is the response with pressure? Can the response for one molecular species be predicted from the known response for another species? How will the response for one species be affected by the pressure of other species? How dependent is the instrument response on instrument control variables?

We have attempted to answer these questions about instrument performance for a group of commercial PPAs. Our objectives were to determine some measure of the range of performance that can be expected from commercial instruments, to highlight particular problems that must be addressed if usable calibration results are to be obtained and, if possible, to discover correlations between design features and performance. Our primary interests in this study were the first of the questions raised in the previous paragraph, i.e., stability, linearity, and the interactions between and the

effects of different gases. However, as it turned out, the last question, "How dependent is the instrument response on instrument control variables?" is a critical question for most of the instruments that we tested. The performance of some instruments was found to be strongly dependent on operating parameters. An initial series of measurements was made to examine the dependence of sensitivity on ion source parameters and peak width. This was followed by an extensive series of measurements to determine the dependence of sensitivity on pressure, for various combinations of ion source parameters. Subsequent tests, performed at a somewhat arbitrary but fixed "base" set of parameters, examined stability of response with time and influence of one gas on sensitivity to another.

Our selection of instruments for this investigation was dictated largely by availability, but we achieved diversity in at least one regard: the cost of the instruments ranged from $7000 to $29 000. Since the market for PPAs has been dominated in recent years by electric quadrupole-type instruments,[1] most of the instruments available to us were quadrupoles, and the five instruments for which we have extensive test results are all quadrupoles.

## II. EXPERIMENTAL APPARATUS AND PROCEDURES

### A. Test instruments

A typical quadrupole gas analyzer is illustrated in Fig. 1. It has three basic sections: an electron-impact ion source, a quadrupole ion filter and an ion detector. The ion source may be any of several different designs but all have four critical variables: the electron emission current; the filament-to-anode voltage, which is the primary factor determining electron energy; the ion extraction voltage, which is a factor in determining ion focusing; and the potential difference between the ion source and the quadrupole axis, which is the primary factor in determining ion speed through the quadrupole filter. Once it has left the source, the probability of an ion passing through the analyzer depends on the dimensions of the analyzer, the relative dimensions of the source and its alignment with the analyzer, the ion energy, the magnitude and frequency of the rf voltage on the analyzer, and the ratio of the dc to the rf voltages. The current generated at the detector by ions passing through the analyzer will depend on the size and alignment of the detector, its surface condition, and, for secondary electron multipliers, the secondary emission efficiency and accelerating voltages of the detector. Principles and applications of quadrupoles, as well as other types of PPAs, are discussed in various review articles.[2-9]

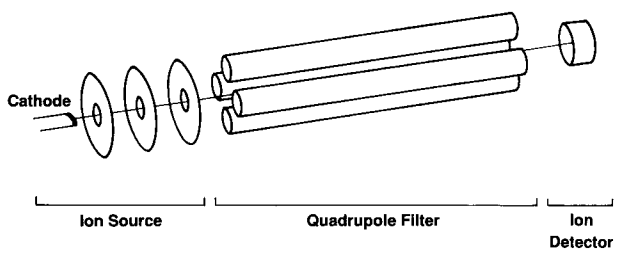


FIG. 1. Typical quadrupole gas analyzer.

Commonly, instrument controls for different operating parameters are identified by descriptive but not entirely accurate names. As an example, the control for the potential difference between the anode (corresponds to the grid or plate in an ionization gauge) and the filament is commonly called "electron energy." While electron energy in the region where the extracted ions are produced is largely determined by this potential, it is also influenced by other factors, e.g., field gradients and space charge. We will maintain the distinction between common terms and physical parameters by the use of the term "control" where appropriate.

The five test instruments are identified by the letters *A–E*, and several design parameters for these instruments are presented in Table I. All instruments were new at the time the tests were started. For some instruments, all of the electrical parameters can be adjusted by the user, in other cases most of them are preset by the manufacturer. The range of adjustment of the ion source parameters is also indicated for the different instruments in Table I. In some cases preferred operating parameters were specified by the manufacturer, in other cases no preference was specified. A single number indicates a preset, and presumably preferred value. The ion sources for the five instruments are illustrated in Fig. 2. In order to minimize variables, it was our original intention to operate all instruments with tungsten filaments, however, two of them were available only with thoria-coated iridium filaments.

All PPAs were operated with their commercial control units. However, for instruments *A*, *B*, *D*, and *E*, ion current measurements were made using a multiplexer and a common digital picoammeter. Ion current in instrument *C* was not directly accessible; for this instrument the digital output of its analog-to-digital converter was recorded. In every case, Faraday cup or plate ion collectors were used; secondary electron multipliers (SEMs) were not used in any of the measurements. The accuracy of the picoammeter was checked with a calibrated current source and its uncertainty is estimated to be 1% or less for all ranges. All uncertainties quoted in this article are at the 99.7% confidence level.

To check the consistency of our results and the performance of the calibration apparatus, two Bayard–Alpert (BA) ionization gauges were tested at the same time and in the same manner as the PPAs. One of the ion gauges was glass tubulated, the other was a nude design. Both had tungsten filaments and were operated at 1 mA electron emission, 30 V filament bias, 180 V grid bias, and the ion collector at ground. The same picoammeter was used for the ion gauge current measurements as was used for the PPAs. It should be noted therefore, that with the exception of PPA *C*, the errors in our results due to noise, drift, and mismatch between measuring ranges of our calibrated digital picoammeter may be less than the corresponding errors associated with the instruments' own ammeters (electrometers).

### B. Calibration apparatus

#### *1. Vacuum system*

The calibration apparatus is illustrated schematically in Fig. 3. The construction, including gas inlet lines, was weld-

TABLE I. Selected test instrument information

| PPA test instrument | *A* | *B* | *C* | *D* | *E* |
|---|---|---|---|---|---|
| Rod length (mm) | 100 | 140 | 114.3 | 220 | 125 |
| Rod diameter (mm) | 6.0 | 6.3 | 6.3 | 19 | 6.3 |
| Field radius (mm)[a] | 2.6 | 2.73 | 2.71 | 8.38 | 2.25 |
| Frequency (MHz) | 2.46 | 2.5 | 2.75 | 1.2 | 2 |
| Ionizer geometry | b | b | b | b | b |
| Filament material | Thoria-coated iridium | Tungsten | Thoria-coated iridium | Tungsten | Tungsten |
| Emission current range (mA) | 0.07–2 | 0.1–1 | 0.1–10[c] | 0.1–30 | 1.45[d] |
| Electron energy range (eV) | 93[d] | 25–70[e] | 30–150[e] | 5–100 | 58[d] |
| Ion energy range (eV) | 0–15 | 0–15[f] | 1–10[g] | 0–100 | 1.6–6 |

[a] Radius of cylinder which can fit inside the quadrupole structure and is tangent to the four rods.
[b] See Fig. 2.
[c] 1 mA recommended by manufacturer.
[d] Value fixed by manufacturer's design.
[e] 70 eV recommended by manufacturer.
[f] 8 eV recommended by manufacturer.
[g] 6–8 eV recommended by manufacturer.

ed stainless steel and metallic demountable seals. The test chamber was a 45 cm diam cylinder, 17 cm high, with instrument test ports welded into the cylindrical wall midway between the top and bottom of the chamber. The test instruments were contained in stainless steel housings mounted to individual test ports with Conflat-type seals. Similarly attached to the chamber were the two BA gauges and a molecular drag gauge (MDG)[10] used in the calibration of the test instruments. The calibration chamber was pumped through a 19 mm diam orifice $L_2$ by a nominal 0.5 $m^3/s$ turbomolecular pump. The basic design of this chamber is similar to the chamber of the National Institute of Standards and Technol-

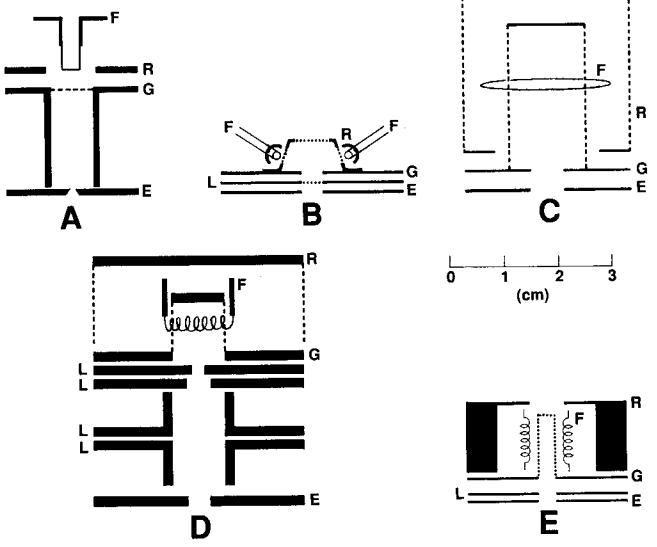


FIG. 2. Test instruments (*A–E*) ionizer geometry, drawn to scale: R = electron reflector; G = grid (anode) for electrons; L = ion lens or focus element; E = entrance plate to quadrupole; F = filament. Note that in instrument *B* both the focus element and the entrance plate were fixed at zero (0) V. Also note that the entrance plate in instrument *D* employs a biased dielectric element and is not quite as simple as that shown.

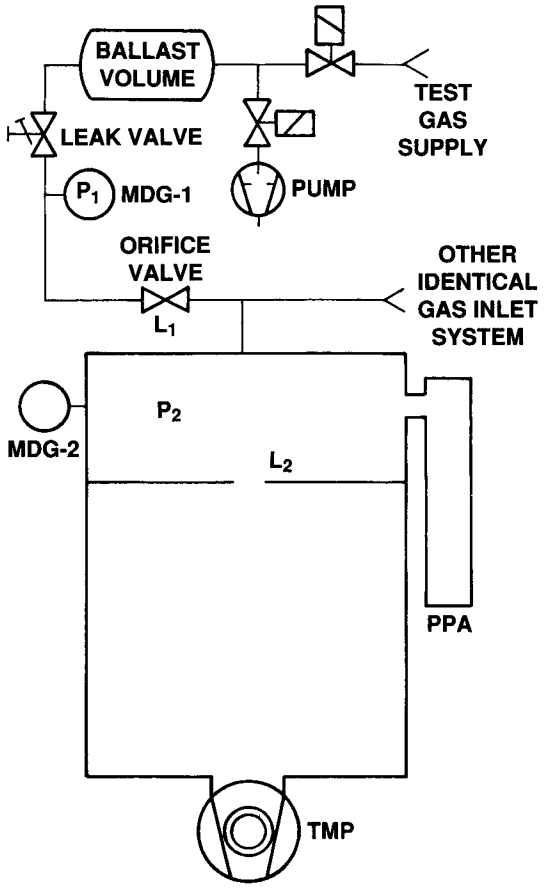


FIG. 3. Schematic diagram of test apparatus. The five test instruments and the two BA gauges were all attached to the calibration chamber above the orifice $L_2$.

ogy primary vacuum standard.[11] Based on experience with that system, the pressures in this chamber are estimated to be uniform to within 0.1%.

### 2. Partial pressure control and measurement

Two independent and identical inlet systems were used to control the partial pressure of test gases. Each inlet system included an eight liter ballast volume, connected through electrically controlled valves to a gas supply cylinder and a mechanical vacuum pump. Following the ballast volumes were all-metal variable-leak valves. After presetting the leak valve, the flow of a particular gas into the calibration chamber and through the orifice $L_2$ could be controlled by adjusting the pressure in the ballast volume. This system allowed the quick establishment of partial pressures of inert gases with instabilities of the order of 0.1%/h. However, for active gases, e.g., $CO_2$, CO, $O_2$, we believe that adsorption phenomena in the calibration chamber caused delays in the establishment of equilibrium pressure that could have time constants of hours at low pressures. Laboratory-grade bottled gases with specified impurities of 0.01% or less were used for most measurements. Their purities and the integrity of the gas inlet systems were qualitatively verified using the PPAs.

The partial pressures were measured using calibrated MDGs in two different ways. In the first of these, partial pressures in the calibration chamber were directly measured using MDG-2 attached to the calibration chamber. This was done for pressures between $10^{-4}$ and $10^{-1}$ Pa, with the lower limit being set by the random errors of the MDG. The second technique employed the MDG mounted in each inlet system upstream from the calibration chamber. Between each MDG and the calibration chamber is an all-metal bakeable valve with a small orifice $L_1$ drilled through the valve seat. With the valve "closed" the pressure $P_1$ upstream from the orifice valve is about 1500 times the pressure $P_2$ in the calibration chamber. The exact value of the pressure ratio was determined from the ratio of the MDG-1 and MDG-2 readings when the system was operated with a pressure of about $10^{-4}$ Pa in the calibration chamber with the valve closed (note that only MDG-2 needs to be absolutely calibrated in this technique). Since the flow through both $L_1$ and $L_2$ is molecular for chamber pressures up to about $2.5\times10^{-3}$ Pa, the pressure ratio will be constant, and the MDG-1 readings, with appropriate viscosity corrections, can be used to predict the calibration chamber pressure for all gases between pressures of about $10^{-7}$ and $2.5\times10^{-3}$ Pa. In practice, this technique was used only for pressures up to about $10^{-4}$ Pa. Above this pressure, MDG-2 on the calibration chamber was used to directly measure the chamber pressure. The two inlet systems allow the determination of the partial pressures of two gases at the same time, independently of one another to within 1%, if the partial pressures are within a factor of 15 of one another.

The three MDGs were calibrated for $N_2$ against the NIST primary vacuum standard,[11] which has a total uncertainty of 1.7%. When measuring other gases with the MDGs, the $N_2$ effective accommodation coefficient was used and a correction was made for the molecular weight. Our experience has shown that the additional uncertainty introduced by this procedure does not exceed 2%. Pressure ratios across the orifices in the valve seats were determined with an uncertainty of 0.3%. From periodic intercomparison of the MDGs, we believe that changes in their calibrations were no larger than 1%. Linearly summing these component uncertainties yields an upper bound of 5% on the systematic uncertainty in the measured pressures. For many of the PPA calibrations, the linearity of an instrument's response was of more interest than the absolute magnitude of its sensitivity. We estimate that the nonlinearity (maximum change in percentage error with pressure) of the MDG pressure measurements, caused by errors in the gas viscosity correction and the pressure ratio, did not exceed 1.5%.

## C. Procedures

### 1. Bakeout

After initial assembly, the entire calibration system, including the inlet system between the leak valves and the calibration chamber, and all test and calibration instruments, was baked at 250 °C for eight hours. The ion sources of the PPAs and the BA gauges were connected to power supplies with Teflon-insulated wire and operated with 1 mA emission during bakeout. To minimize transport of tungsten from the filaments to the surrounding insulators, the filament heating should be started after the majority of adsorbed $H_2O$ in the system has been driven off by baking and pumped away. We have found that this procedure gives a lower indicated base pressure and a "cleaner" residual gas spectrum than obtained with the use of conventional heated-grid outgassing. No further outgassing of any of the instruments was done. After bakeout, the residual gas spectrum was dominated by a $H_2$ peak, with the next largest peak due to CO. Indicated base pressures were about $10^{-8}$ Pa, true $H_2$ pressure.

### 2. Test measurements

Most of the test measurements were a series of calibrations with pure gases for different values of operating parameters. Each calibration started at base pressure where offset corrections for the MDGs were determined and any necessary adjustments made to the test instruments. The data started with a calibration pressure of about $10^{-7}$ Pa and proceeded with increasing pressures to about $10^{-1}$ Pa, with typically six calibration points per decade. In some cases, calibration data were taken for decreasing pressures as well, in order to determine instrument hysteresis. In all cases, for each calibration pressure, data for all of the PPAs and the BA gauges were taken simultaneously, to within the 100 s required to scan the common picoammeter through the instruments. This allowed independent verification that any anomalous behavior observed was due to the particular instrument rather than a malfunction of the calibration apparatus.

Another important series of calibrations involved the determination of the effect of a matrix gas on the sensitivity to a test gas. For these measurements, a partial pressure of the test gas, typically $10^{-6}$ Pa, was established, measured, and maintained at a constant value using one inlet system. The offset correction of the MDGs in the calibration chamber

and the other inlet system were then determined, so that the constant test-gas pressure was part of the offset correction. Using the second inlet system, the matrix gas pressure was then varied as appropriate, while measurements were made of the test-gas signal.

Data acquisition was computer controlled, and all data were stored on magnetic disks for subsequent analysis. The partial pressures could be automatically changed by computer control of pneumatically actuated valves connecting each ballast volume to a gas supply bottle or a vacuum pump. This permitted data acquisition on a 24 h/day basis, manual intervention being required only to change PPA control parameters or gas supply bottles.

## III. RESULTS AND DISCUSSION

In many reports, PPA or ion gauge calibration results are presented as plots of the logarithm of the ion current versus the logarithm of the pressure. Unfortunately, this type of presentation can obscure significant nonlinearities. Therefore, we choose to present our results in terms of sensitivity $S$ defined as the ratio of the change in detected ion current to the corresponding change in partial pressure of a particular species $x$.

$$S(x) = [I(x) - I_0(x)]/[P(x) - P_0(x)]. \quad (1)$$

$I(x)$ is the ion current at partial pressure $P(x)$ when the instrument is tuned to the molecular peak of species $x$, and $I_0(x)$ is the corresponding value at some reference pressure $P_0(x)$, generally the base pressure of the system. Note that this definition differs from that commonly used for ion gauge sensitivity in that the change in the ion current is not divided by the electron emission current. As will be shown, the sensitivity of any instrument is, in general, not constant, as it may depend on a number of variables including molecular species and time and history of use, as well as pressure and the operating parameters of the instrument.

In discussing the behavior of instrument response as a function of time, the notion of a base sensitivity, $S_b$, is useful. The base sensitivity is defined here as the sensitivity of an instrument for a particular species, pressure, and set of operating parameters. For purposes of this study, the base sensitivity was that determined for argon at a pressure of $10^{-4}$ Pa. Where the operating controls could be adjusted, they were set for 1 mA electron emission current, 60 eV electron energy, and 5 eV ion energy. The peak width $\Delta M$ was adjusted to 1 amu at mass-to-charge ratios $M/Q$ of 4 and 40. For instruments with focus electrodes, the focus voltage was adjusted for maximum ion current. For instruments with fixed parameters the values are those listed in Table I. As will be discussed, the sensitivity of the instruments varied significantly with time and operating conditions. However, allowing for these variations, there were large differences between the sensitivities of the instruments. For example, with Faraday cup ion detection, the maximum argon sensitivity achieved by adjusting ion energy at base operating conditions at $10^{-4}$ Pa, were (in units of $10^{-7}$ A/P) 2.2, 5.0, 19, 26, and 52 for PPAs *D*, *B*, *E*, *C* and *A* respectively.

### A. Dependence of sensitivity on operating controls

As previously noted, the performance of a PPA depends on a number of operating parameters. No one set of parameters is optimum for all applications or all instruments. Therefore, it is desirable to understand the relationship between these parameters and instrument performance. In many cases, as shown below, these relationships will be quite different for different instruments. The control functions of different instruments are in general similar, but different names may be used for the same control by different manufacturers. We have tried to use the most common designations.

The electron energy control establishes the dc potential between the cathode (filament) and anode. The ion energy control establishes the difference between the dc potential of the quadrupole axis and an electrode in the ion source. The actual electron or ion energies may differ somewhat from the control values because of space charge effects.

Note that at least two definitions of the resolving capability of an instrument are in common use. The definition employed here is the peak width $\Delta M$, at 10% of the peak height. Peak width is approximately independent of mass-to-charge ratio for a typical quadrupole adjustment. The peak width is commonly adjusted by two variables: a dc offset on the quadrupole rods and the ratio of the variable rf to dc voltages on the rods. The first of these most strongly affects the peak width at low charge-to-mass ratios, the second the peak width at higher masses. Controls for these two adjustments are often referred to as resolution low and resolution high. During these tests the resolution-low control was adjusted to obtain a peak width of 1 amu at a mass-to-charge ratio of 4. The resolution-high control was similarly adjusted at mass-to-charge ratio 40. In Secs. III A 1–III A 4 below, we discuss the influence of instrument controls on the sensitivity at a constant partial pressure of $10^{-4}$ Pa.

#### *1. Electron emission*

Figure 4 illustrates the correspondence between indicated electron emission current and the detected ion current for four of the instruments at an argon partial pressure of $10^{-4}$ Pa. (Emission current was not adjustable in instrument *E*.) All of the instruments were operated with the base set of parameters except, of course, for the electron emission. The data shown in Fig. 4 were chosen to illustrate the range of behavior possible with different PPAs. Although changing the pressure, the gas, the ion energy or the electron energy will result in characteristics different from those shown, the characteristics differed from instrument to instrument more than they did with these other variables. It is apparent also, that PPAs do not necessarily show the proportional ion current versus electron current relation that is expected for ion gauges (although ion gauges are not always strictly linear either).

We believe that the quite different behaviors illustrated in Fig. 4 can be correlated with the different ion source designs (refer to Fig. 2). Instrument *C* is the only one to show a linear behavior over an extended range. Its ion source is an open ("nude" or "grid") structure somewhat similar to the

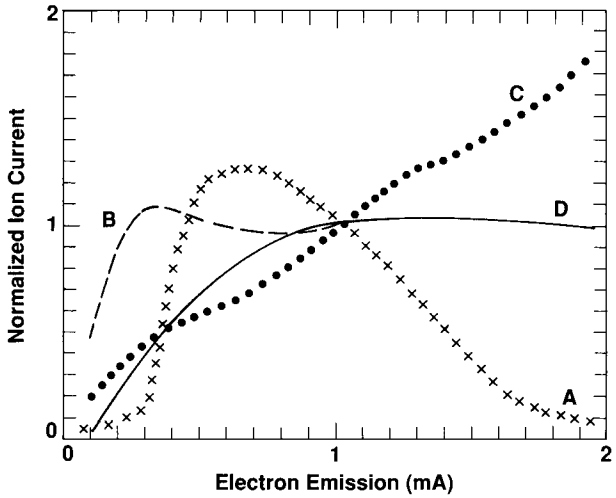


FIG. 4. $Ar^+$ ion current vs electron emission current for PPAs *A*, *B*, *C*, and *D* at $10^{-4}$ Pa argon pressure, 60 eV electron energy (93 eV for PPA *A*), and 5 eV ion energy. (Emission not adjustable in PPA *E*.) Ion current was normalized to a value of 1 at $I_e = 1$ mA.

filament and grid structure of a BA ion gauge. Instrument *A*, whose characteristic is not even monotonic, let alone linear, has a very bright and compact source, with the filament positioned on the axis of the instrument. A possible qualitative explanation for its behavior (the maximum in the ion current versus emission current relation) is the following: increasing the electron current in this source at first increases the number of ions produced, but eventually the increasing electron space charge modifies the field created by the source electrodes. This may then decrease the ion draw-out efficiency to the point that there is a decrease in the overall ion yield of the source. Instrument *D* has a compact grid source, intermediate in size and design between those of *A* and *C*. The ionizer in instrument *B* is designed to produce a relatively concentrated wedge-shaped electron beam directed perpendicular to the instrument's axis. The very weak dependence of ion current on emission current above 0.3 mA in instrument *B*, and above about 1 mA with instrument *D*, may also be due to the effects of electron space charge at higher emission currents.

When lacking detailed information on the ion current vs emission current relation for a particular instrument, an unsuspecting user might select a "high" (e.g., 2 mA) electron emission current for low pressure work ( $< 10^{-4}$ Pa) on the assumption that this would assure a high sensitivity. As can be seen in Fig. 4, this is not necessarily the case for all PPAs. Another influence in the selection of emission current is the assumption that reducing the emission current will enhance the linearity with presssure. As the data in this paper will show, this is true for some instruments but not for others.

Two secondary factors will also influence the choice of emission current: filament life and degradation of insulators. If the filament life is determined by evaporation rather than by chemical attack,[12] which is generally the case in baked UHV systems where the partial pressure of water is low, filament life will depend strongly on emission current. A rule of thumb for tungsten filaments is that, at usual emission temperatures, a 10% increase in operating temperature will reduce the filament life by about a factor of 2 and increase the emission current by almost a factor of ten. Rhenium[13] and thoria-coated iridium[14] are other frequently used filament materials. With these materials, the same electron emission can be obtained at lower temperatures than with tungsten, thus reducing the outgassing of the source and reactions with active gas constituents ($O_2$, $H_2O$, and $H_2$). Note that the filament temperature required to achieve a given emission current will depend on the electron accelerating voltage (electron energy control). Generally, to maintain a given emission current, operation with low electron energies will require higher filament temperatures.

The evaporation or other transport of the filament material affects not only the filament lifetime, but may also slowly degrade the performance of the ionizer by depositing conducting layers on insulators. This can cause emission current or source voltages to differ from nominal set values. Because this is a gradual process, changes in PPA performance may not be readily apparent. They can be detected by occasional resistance checks of the insulators. More information on filament materials and on filament-sample interactions can be found in Ref. 15, and in Refs. 16 and 17, respectively.

### 2. Electron energy control

The electron impact ionization cross section for most molecules and atoms increases with electron energy up to a maximum around 100 eV.[18] Other factors remaining the same, the sensitivity of a PPA will increase with increasing ionization cross section. However, as can be seen in Fig. 5, the sensitivity may depend on electron energy in a manner quite different from that predicted by the cross section energy dependence alone. The data in Fig. 5 are for argon at a pressure of $10^{-4}$ Pa; the PPAs were operated at 1 mA emission and a 5 eV ion energy control setting. The peak sensitivity for instruments *C* and *D* occurred well below 90 eV, where the argon ionization cross section is a maximum.[18] Sensitivity for instrument *B* monotonically decreased with increasing electron energy control, starting as low as the minimum setting of 30 eV.

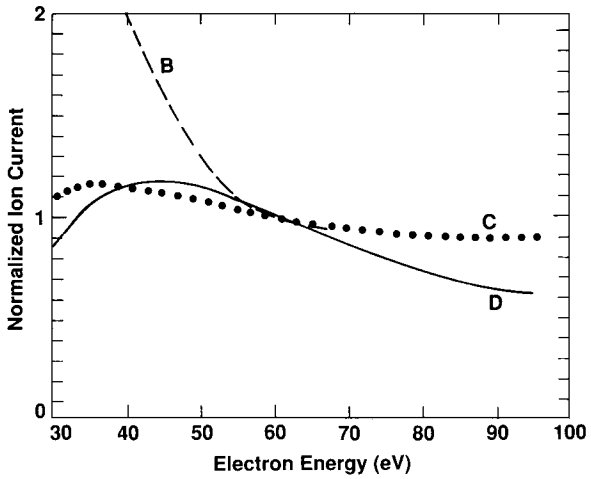


FIG. 5. $Ar^+$ ion current vs electron energy control for PPAs *B*, *C*, and *D* at $10^{-4}$ Pa argon pressure, 1 mA emission current, and 5 eV ion energy. (Electron energy not adjustable in PPAs *A* and *E*. See Table I.) Ion current was normalized to a value of 1 at $E_e = 60$ eV.

We do not understand these performance differences among the test instruments. As shown in Fig. 2, the ionizer geometries of instruments *B*, *C*, and *D*, although not identical, do not appear to differ in any fundamental way. Also, the proportions and length of the quadrupole filter is somewhat different in each instrument (see Table I). Presumably, the differences in behavior arise from competing influences of electron and ion space charge on the ion energies as they enter the quadrupole filter. It is worth noting that cross section measurements are carried out at much lower emission currents than usual in partial pressure analysis ($<0.1$ mA)[19] in order to avoid electron beam space charge effects, and to assure that ion extraction efficiency is independent of the electron energy.[20]

Another consideration when choosing electron energy is molecular fragmentation. Selecting a lower electron energy will reduce fragmentation. This is not necessarily desirable. The spectrum of molecular fragments (the cracking pattern) may help in identifying molecules whose molecular peaks cannot be resolved. As examples, most PPAs cannot resolve the molecular peaks of CO and $N_2$, or those of $CO_2$ and $N_2O$, but their cracking patterns are quite different and may be used to resolve the ambiguities in the molecular peak.

As pointed out above, electron energy control will also affect filament temperature: to maintain a given emission current, the filament temperature must be increased as the electron accelerating voltage is reduced. Filament temperature can be minimized by using the lowest emission current required and the highest electron energy.

### 3. Ion energy control

The data in Fig. 6 were obtained by varying the ion energy control with other parameters at the "base" values and constant argon pressure of $10^{-4}$ Pa. Peak width, which depends on the rf/dc ratio as well as ion energy, was not held constant. The rf/dc ratio control (sometimes known as "resolution high") was initially adjusted to obtain a peak width of $\Delta M = 1$ amu at $M/Q = 40$ for an ion energy control setting of 5 eV. Thereafter, the rf/dc ratio control remained fixed at that setting. As can be seen in Fig. 6, the sensitivity of each test instrument increased with ion energy control. The steady increase of the sensitivity with ion energy has led at least one manufacturer to call this control the "sensitivity control".

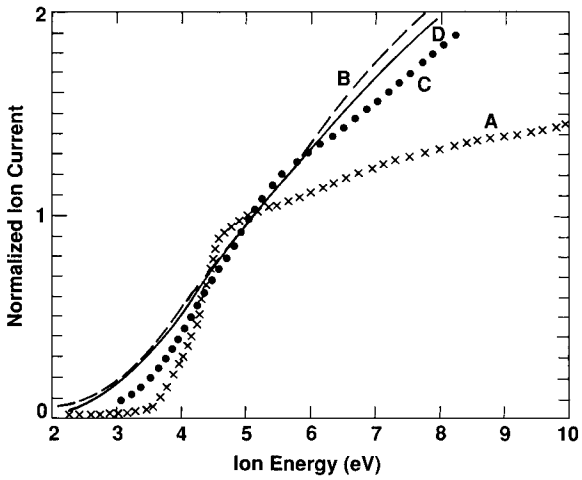


FIG. 6. $Ar^+$ ion current vs ion energy control for PPAs *A*, *B*, *C*, and *D* at $10^{-4}$ Pa argon pressure, 1 mA emission current, and 60 eV electron energy (93 eV for PPA *A*). Ion current was normalized to a value of 1 at $E_i = 5$ eV.

In the analytical treatment of an ideal instrument (very long rods and no fringing fields at entrance and exit), the filtering action of the quadrupole is independent of the ion's speed, provided it is not too fast.[21] Nevertheless, as shown in Fig. 6 and as reported by Brubaker[22] and Austin *et al.*,[23] there is a strong correlation between sensitivity and ion energy. This correlation appears to be due to two factors. First, as the ion energy is increased, the angular distribution of ions leaving the source (angular emittance) is narrowed, resulting in a better match with the acceptance of the analyzer. Second, as the ion energy increases, the ions spend less time in the fringe fields between the source and the analyzer, with a consequent reduction in ion loss associated with this region.[24] We believe that the nonlinear behavior for instrument *A* compared to the other instruments, may arise from a relatively high space charge in its ion source. Data taken at 0.1 mA electron emission, as opposed to the 1 mA used for the data in Fig. 6, yielded a much more linear sensitivity versus ion energy relation. Some dependence of sensitivity on the ion source space charge can be expected since the energy of an ion is, as noted before, not just dependent on the ion energy control, but rather is determined by the total potential difference between the ion formation region and the axis of the quadrupole, including the effect of space charge.

### 4. Peak width

As noted before, peak width $\Delta M$ (sometimes called "resolution") depends on both ion energy and the rf/dc ratio on the quadrupole rods. The rf/dc ratio has the major effect on peak width since this parameter determines the range of $M/Q$ values for which ions perform bounded oscillations in the quadrupole field. On the other hand, as the ion energy is increased at fixed rf/dc ratio, the ions spend less time in the fringing fields at the entrance and exit of the quadrupole and therefore a larger fraction of the selected ions reach the detector, with little change in peak width. As an example, consider the data shown in Fig. 7. The filled circles represent measured values of $Ar^+$ ion signal and peak width for instrument *D* at an argon pressure of $10^{-4}$ Pa. The influence of both the rf/dc ratio and the ion energy on the relation between ion current and peak width in this instrument is shown by the two families of curves. The solid lines connect the data points obtained by varying the ion energy control at fixed resolution control (rf/dc ratio) settings (indicated by the letters *a*–*g*). The complementary dotted lines connect data points corresponding to a constant value of ion energy. A similar family of curves, plotted against reciprocal peak width, is shown in Fig. 6.17 of Ref. 21.

Usually, there is another control influencing the peak width—the dc offset or "resolution low"—which has a large effect on the lower masses ($H_2$, He). The usual mode of operation is to adjust for more or less constant peak width over the entire mass range.[25] This adjustment results in reduced transmission at higher masses.[26] The adjustment also

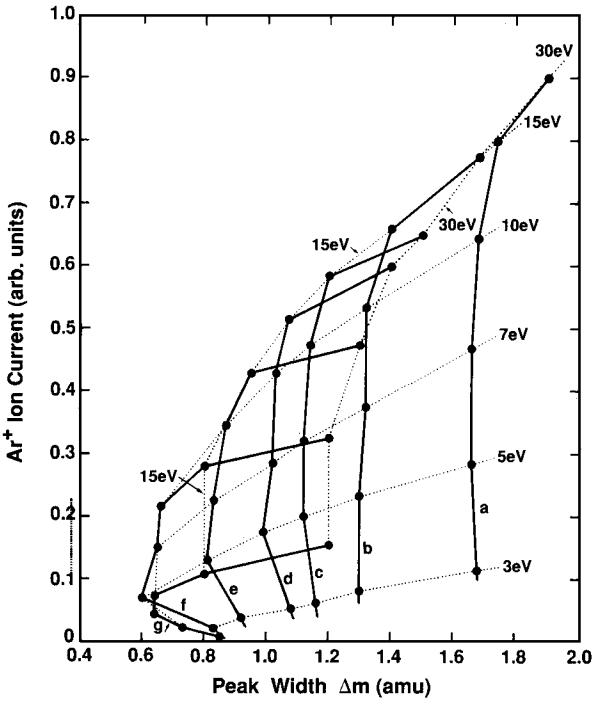


FIG. 7. Influences of both ion energy (eV) and rf/dc ratio on relationship between $Ar^+$ signal and peak width $\Delta m$ in PPA $D$ at $10^{-4}$ Pa argon pressure. Solid curves labeled $a$ through $g$ correspond to seven different settings of the rf/dc ratio control; dotted curves correspond to constant ion energy. Ion currents are all scaled by the same factor, somewhat arbitrarily chosen, to make the largest current have a value of 0.9.

can have a significant effect on the relative sensitivities for different gases. For example, by adjustment of the resolution-high and resolution-low controls in instrument $D$, the ratio of the peak heights of the $He^+$ and $Ar^+$ signals developed from a 1:1 Ar/He mixture could easily be made to vary from 1:9 to 9:1.

## B. Dependence of sensitivity on gas species

As in the case of ion gauges, for a given instrument it is convenient to express its sensitivity for a specific gas as a relative sensitivity, i.e., as the ratio of its absolute sensitivity for this gas to its absolute sensitivity for a reference gas, in this case argon.[27] In the preceding section it was mentioned that, for a given PPA, relative sensitivity for different gas species can be varied significantly by adjustment of its resolution-high and resolution-low controls. However, even if these controls are adjusted in the same manner for different instruments, i.e., if the instruments are each adjusted for peak widths of 1 amu at mass-to-charge ratios of 4 and 40, significant differences are observed in the relative sensitivities of different instruments as a function of gas species. Table II shows the sensitivity values relative to argon for different gases measured at the molecular ion peak and base parameter set ($I_e = 1$ mA, $E_e = 60$ eV, $E_i = 5$ eV, and $\Delta M = 1$ amu). Note that these values differ significantly from one instrument to another, and in many cases they differ significantly from various tabulated values for ionization gauges.

There are a number of factors that can cause this variability. The relative sensitivity for different gases depends on the fragmentation factor, the ionization probability relative to argon, the transmission factor and the detection probability, also relative to argon. The fragmentation factor[28] for a particular ionic species is the ratio of ion current measured for that ion species to the sum of ion currents measured for each of ionic species produced from the parent molecule (the cracking pattern). Cracking patterns are tabulated in manuals or can be found in the literature.[26,29,30] However, as noted before, the cracking pattern and fragmentation factors depend on the electron energy. The fragmentation factor also depends on the construction of the source and on the source parameter adjustments. Therefore, tabulated fragmentation factors should be relied upon only for qualitative analyses or compound identification. The transmission factor covers the acceptance and discrimination of the filter[31,32] and so depends mainly on the resolution settings and the ion energy. The detection probability is effectively invariant for different species for Faraday cup detectors, but SEM gain may depend considerably on ion species.[33,34]

## C. Linearity of ion current with partial pressure

For many applications, a nearly linear relation between ion current and partial pressure is highly desirable. A linear response simplifies the calibration of a PPA since the sensitivity need not be determined over the entire pressure range, and even the analysis of relative partial pressures will be simplified if corrections do not have to be made for the pressure dependence of relative sensitivities. We have investigated the influence of several factors on the linearity.

### 1. Operating parameters

We have investigated the influence of operating parameters on linearity by calibrating each of the instruments with argon over the pressure range $10^{-7}$ to $10^{-1}$ Pa, for different combinations of operating parameters. Specifically, except in cases where the operating parameter could not be adjusted, each instrument was calibrated for electron emission currents of 0.5, 1, and 2 mA; electron energy control settings of 30, 60, and 100 eV; and ion energy control settings of 3, 5, and 10 eV. The 27 different calibrations obtained for each of the five instruments revealed a wide range of behavior.

We attempt to illustrate this range of behavior for each of the five instruments in Figs. 8–12. Of the 27 data sets for each PPA, three different sets of data have been selected: an example showing nonlinearity at low pressure (if the instrument exhibited such behavior), plotted with filled circles; an example showing nonlinearity at high pressure, plotted with filled squares; and, the most nearly linear data set, plotted as a continuous line without a plotting symbol. To facilitate comparison of nonlinearity, each set of data has been normalized to a value of 1 at $10^{-4}$ Pa. In each figure, part of the data set showing nonlinearity at high pressure has been scaled by the factor indicated in the plot.

From these plots it is apparent that there are significant differences in the nonlinearities for the different instruments. These differences are even more apparent from an examination of the entire set of 27 calibrations for each in-

TABLE II. Sensitivities, relative to argon, determined in this work for the five PPA test instruments and the two ion gauges; $T$ = tubulated BAG, and $N$ = nude BAG. All sensitivities were determined using the molecular ion (for example, $CH_4^+$ for $CH_4$). All PPA ionizers were operated at, or as close as possible to, the "base" parameter set: $I_e = 1$ mA, $E_i = 5$ eV, and $E_e = 60$ eV. Resolution controls were adjusted to obtain $\Delta M = 1$ amu at $M/Q = 4$ and 40.

| | Test Instruments | | | | | | |
|---|---|---|---|---|---|---|---|
| | Partial pressure analyzers | | | | | Ion gauges | |
| Gas species | *A* | *B* | *C* | *D* | *E* | *T* | *N* |
| Ar | 1.00 | 1.00 | 1.00 | 1.00 | 1.00 | 1.00 | 1.00 |
| $CH_4$ | 0.60 | 0.72 | 0.79 | 0.37 | 0.70 | 1.08 | 1.15 |
| $CO_2$ | 0.75 | 0.58 | 0.89 | 0.73 | 0.76 | 1.02 | 1.10 |
| $N_2O$ | 0.65 | 0.35 | 0.58 | 0.43 | 0.51 | 0.98 | 1.06 |
| CO | 0.53 | 0.74 | 0.67 | 0.48 | 0.80 | 0.70 | 0.72 |
| $N_2$ | 0.51 | 0.75 | 0.64 | 0.48 | 0.81 | 0.69 | 0.70 |
| $H_2$ | 0.31 | 0.82 | 0.91 | 0.15 | 1.25 | 0.31 | 0.28 |
| He | 0.05 | 0.26 | 0.20 | 0.23 | 0.32 | 0.13 | 0.13 |

strument. For PPA *D*, the examples of nonlinearity shown in Fig. 11 as circles and squares could be obtained only for extreme choices of the ion and electron energy. As shown in Figs. 13 and 14, for most choices of operating parameters, the nonlinearity in instrument *D* was relatively small and very close to that illustrated by the data for the "most linear" case. On the other hand, the nonlinearities at high and low pressure illustrated for PPA *A* were observed for a wide range of its operating parameters, and the most linear case was a best compromise between these two extremes. Figure 15 shows the marked influence of electron emission current on linearity in PPA *A*.

We have tried to correlate features of the observed behavior with different combinations of operating parameters. There seemed to be no inviolable rules, but certain qualitative trends could be recognized. For example, in all the instruments except PPA *C*, electron energy had a relatively weak influence on linearity in comparison with ion energy and electron emission. Two of these trends appear to be particularly noteworthy.

(a) A maximum in the sensitivity tended to develop in the $10^{-3}$–$10^{-1}$ Pa pressure range whenever an instrument was operated at "low" ion energy. This is illustrated in Fig. 16. The height of this sensitivity maximum increased with electron emission current and electron energy (refer to Figs. 13 and 14, for example). The magnitude of the increase in sensitivity exhibited by some instruments, relative to their sensitivity at $10^{-4}$ Pa, was surprising, becoming as large as a factor of 100 for instrument *A* (see Fig. 8). This sensitivity maximum at high pressure has often been observed for PPAs and ion gauges,[28,35–38] and has been attributed to space charge effects.

(b) A gradual decrease of sensitivity with increasing pressure, without the development of a sensitivity maximum, was evident in four of the test instruments when operated at "high" ion energy. This is illustrated in Fig. 17. A particular-

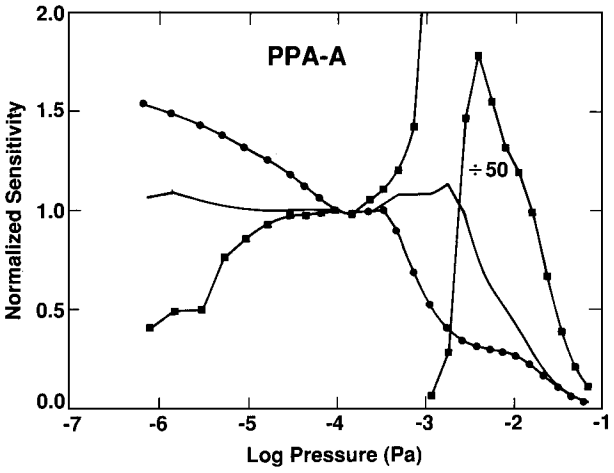


FIG. 8. Examples of Ar sensitivity vs pressure for PPA *A*. Data shown as solid squares correspond to $I_e$(mA)/$E_e$(eV)/$E_i$(eV) = 2/93/3; solid circles 0.5/93/10; smooth curve 1/93/10. Sensitivities are normalized to a value of 1 at $10^{-4}$ Pa.

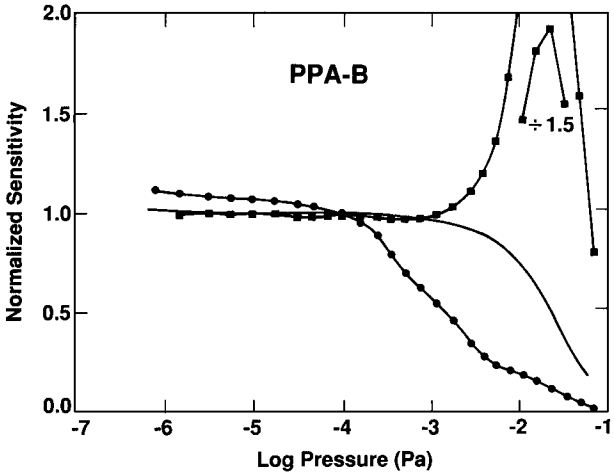


FIG. 9. Examples of Ar sensitivity vs pressure for PPA *B*. Data shown as solid squares correspond to $I_e$(mA)/$E_e$(eV)/$E_i$(eV) = 1/80/3; solid circles 1/30/10; smooth curve 0.5/60/10. Sensitivities are normalized to a value of 1 at $10^{-4}$ Pa.

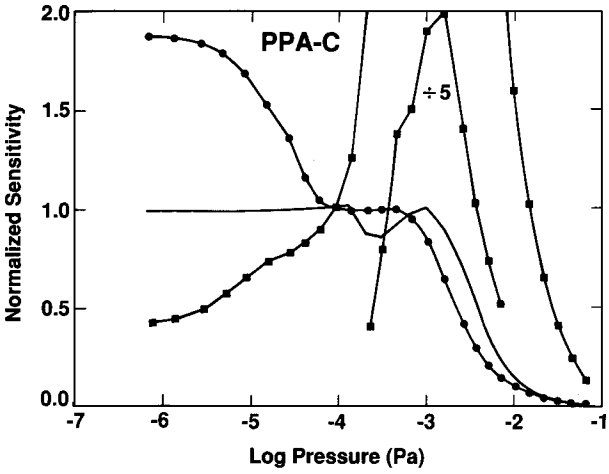


FIG. 10. Examples of Ar sensitivity vs pressure for PPA *C*. Data shown as solid squares correspond to $I_e$(mA)/$E_e$(eV)/$E_i$(eV) = 2/100/3;solid circles 2/100/10; smooth curve 0.5/60/10. Sensitivities are normalized to a value of 1 at $10^{-4}$ Pa.

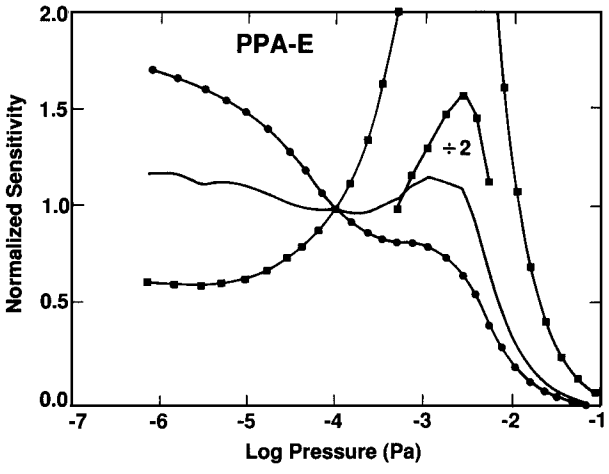


FIG. 12. Examples of Ar sensitivity vs pressure for PPA *E*. Data shown as solid squares correspond to $I_e$(mA)/$E_e$(eV)/$E_i$(eV) = 1.45/58/3; solid circles 1.45/58/5; smooth curve 1.45/58/4. Sensitivities are normalized to a value of 1 at $10^{-4}$ Pa.

ly puzzling aspect of this behavior is that the onset of this decline in sensitivity could occur at quite low pressures: the argon data shown in Fig. 17 indicate a continual sensitivity decrease with increasing pressure, for pressures greater than about $10^{-7}$ Pa for instrument *A*, above about $10^{-6}$ Pa for instrument *E*, and above about $10^{-5}$ Pa for instrument *C*. A significant nonlinearity is evident for PPA *B* above about $10^{-4}$ Pa. The behavior of instrument *D* at high ion energy was exceptional. Over the range $10^{-6}$ to $10^{-3}$ Pa, its sensitivity varied by no more than $\pm$ 3.5% from its average value.

Without a detailed analysis of the potential distribution in the ion formation region at high and low ion energy operation, as well as the effect of space charge on this distribution, we can only speculate about the causes of these observed effects. However, the fact that in all five test instruments the detected ion current increased with ion energy (see Fig. 6, data obtained at fixed pressure of $10^{-4}$ Pa) *suggests* an explanation in the case of the sensitivity maximum at high pressure, which occurred when the instruments were operated at low ion energy (see Fig. 16), but was greatly reduced or absent at higher ion energies (see Fig. 17). Referring to Fig. 6, we see that with low ion energy operation (say $E_i$ = 3 eV), a given incremental increase $\Delta E_i$ in ion energy (say $\Delta E_i \approx 1$ eV) will produce a much larger (percentage) increase in detected ion current than the same energy increment at high ion energy (say $E_i$ = 10 eV). We *speculate* that the sensitivity maximum observed at high pressure during low ion energy operation is the result of such an incremental increase in ion energy produced by a positive ion space charge which increases with pressure and raises the potential difference between the ion formation region and

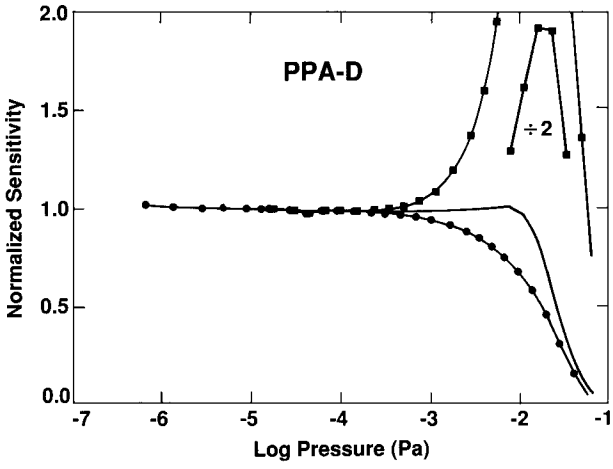


FIG. 11. Examples of Ar sensitivity vs pressure for PPA *D*. Data shown as solid squares correspond to $I_e$(mA)/$E_e$(eV)/$E_i$(eV) = 2/100/3;solid circles 0.5/60/10; smooth curve 1/100/10. Sensitivities are normalized to a value of 1 at $10^{-4}$ Pa.

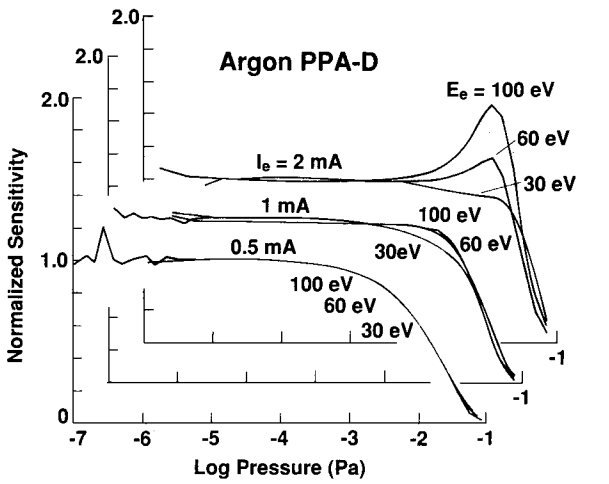


FIG. 13. Ar sensitivity vs pressure for PPA *D* at several different combinations of electron energy $E_e$ and electron emission current $I_e$. Ion energy fixed at $E_i$ = 5 eV. Sensitivities are normalized to a value of 1 at $10^{-4}$ Pa.

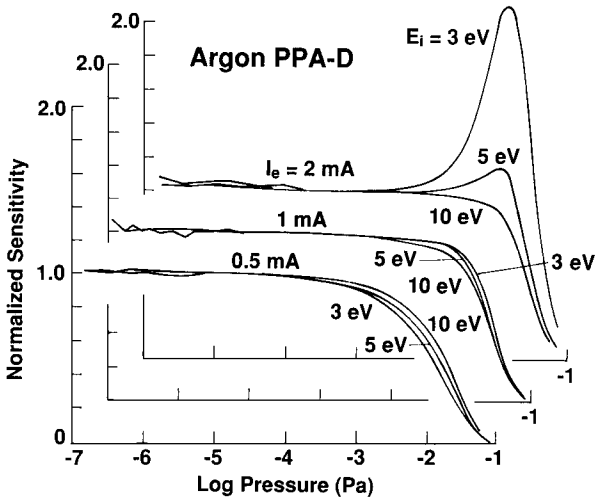


FIG. 14. Ar sensitivity vs pressure for PPA *D* at several different combinations of ion energy $E_i$ and electron emission current $I_e$. Electron energy fixed at $E_e = 60$ eV. Sensitivities are normalized to a value of 1 at $10^{-4}$ Pa.

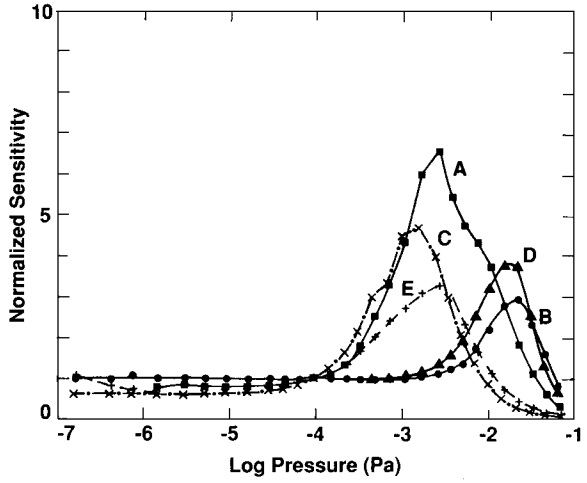


FIG. 16. Examples of the sensitivity maximum (in argon) exhibited by each instrument at low ion energies (2–3 eV). Electron emission current and electron energy at 1 mA and 60 eV, respectively, except $I_e = 1.45$ mA and $E_e = 58$ eV for PPA *E*, and $E_e = 93$ eV for PPA *A*. Each sensitivity curve is normalized to a value of 1 at $10^{-4}$ Pa.

the quadrupole axis. The particularly large sensitivity increase observed in the case of PPA *A* (see Figs. 8 and 16) is consistent with the very large fractional change in ion current with ion energy in the vicinity of $E_i = 3$ eV for PPA *A* (Fig. 6). For all instruments, at sufficiently high pressure, sensitivity begins to decline with further increase in pressure because of ion loss due to recombination and ion-molecule scattering. The relatively small magnitude of the sensitivity increase for some PPAs would seem to imply that their ionizer design reduces the influence of space charge on ion energy.

Unfortunately, at this time we are unable to construct even a speculative explanation for the other effect described above in section (b) (viz., the gradual sensitivity decline with pressure at high ion energy). We believe that to gain a fundamental understanding of these effects, it will be necessary to combine an analysis of the potential distribution in the ionizer with experimental determination of the energy and velocity distribution of the ions as they exit the ionizer and enter the quadrupole.

### 2. Gas species

The dependence of linearity on gas species was evaluated by performing calibrations with different inert gases. Ion source parameters were deliberately selected to produce nonlinearities at either high or low pressures. As can be seen in Fig. 18, the nitrogen results obtained with PPA-*C* at low ion energy are very close to those obtained for argon. For helium however, the deviations from linearity start at a significantly higher pressure than for argon and nitrogen. These results appear to be correlated with positive ion space charge formation. With helium, the same magnitude of ion

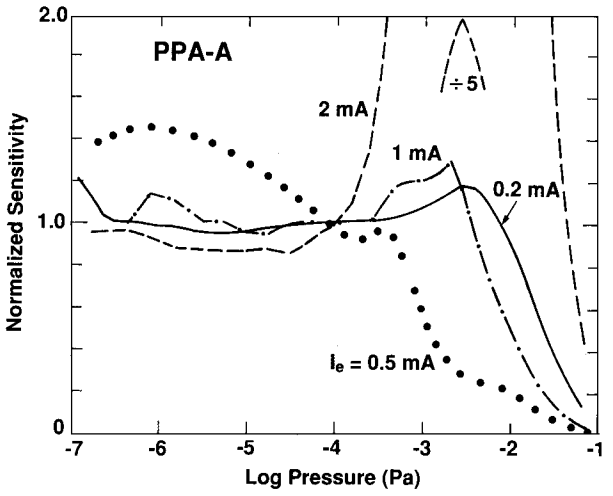


FIG. 15. Influence of electron emission current on linearity of PPA *A*'s response to Ar. Electron and ion energies fixed at $E_e = 93$ eV and $E_i = 5$ eV. Sensitivities are normalized to a value of 1 at $10^{-4}$ Pa.

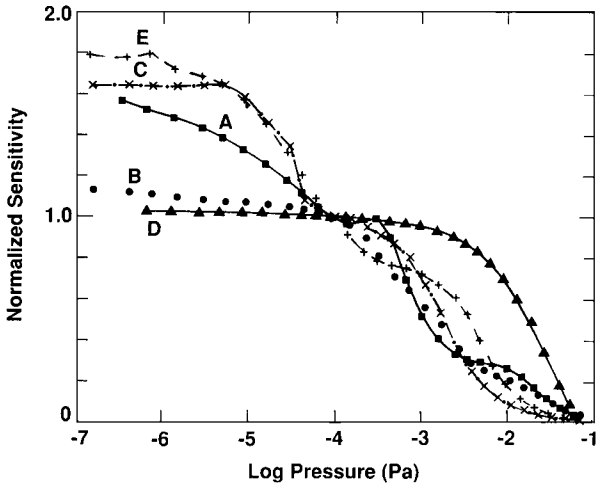


FIG. 17. Examples of nonlinear pressure response in argon at low pressure. Each curve is normalized to a value of 1 at $10^{-4}$ Pa. Ion source parameters for instruments *A* through *E* were $I_e$(mA)/$E_e$(eV)/$E_i$(eV) = 0.5/93/10, 1/30/10, 2/60/10, 0.5/60/10, and 1.45/58/6, respectively.

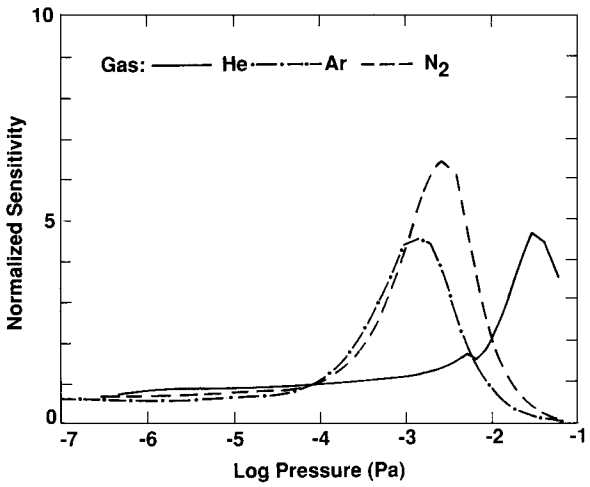


FIG. 18. Influence of gas species on high pressure nonlinearity in PPA *C*. Each curve is normalized to a value of 1 at $10^{-4}$ Pa. Ion source parameters set at $I_e(\text{mA})/E_e(\text{eV})/E_i(\text{eV}) = 1/60/3$.

space charge is expected to be formed at about an order of magnitude of higher pressure than in argon because the helium ionization cross section is about one tenth that for argon. Figure 19 shows the corresponding "high" ion energy results obtained with PPA *E*, an instrument which exhibited nonlinearity at low pressure (see Ar results in Figs. 12 and 17.) In this example, the degree of nonlinearity, especially at low pressure, is significantly smaller with He than for $N_2$ or Ar. Unlike the results shown in Fig. 18, the pressure dependence of the sensitivity is significantly different for each gas, and a simple shift along the pressure axis will not bring the He results into coincidence with the $N_2$ or the Ar results. Linearity measurements were attempted with noninert gases as well (CO, $CO_2$, $H_2$, $N_2O$, and $CH_4$), but considerable difficulties arose as will be discussed in the next section.

### 3. Hysteresis

For a given partial pressure, the ion signal developed in a PPA may depend, to a significant extent, on the pressure history of the instrument. This effect, when it arises from the influence of gas exposure on the instrument's *sensitivity* will be referred to as *hysteresis*. However, examination of this effect can be complicated by long-time-constant transient behavior in the pressure as a result of adsorption/desorption phenomena in the vacuum chamber and attached instruments. Hysteresis was investigated as follows: for each test gas, the instruments' sensitivities were determined at about five pressures per decade, starting at about $10^{-7}$ Pa and increasing to a maximum pressure between $10^{-4}$ and $10^{-1}$ Pa at a rate of about one decade per hour (the "up" path). The calibration pressures were then reduced back down to $10^{-7}$ Pa at about the same rate (the "down" path), again with sensitivities determined at about five points per decade. At any given pressure, a difference between the sensitivity determined along the down path and along the up path is evidence of a possible hysteresis in the instrument.

In Ar, He, and $N_2$, differences between the up and down sensitivity measurements were most pronounced in instruments *A* and *B*, and relatively very small in PPA-*D*. For maximum pressure excursions greater than about $10^{-4}$ Pa, significant up–down differences were quite evident in PPA-*A* and PPA-*B*, as soon as the pressure was reduced below the maximum value, and these differences in sensitivity persisted as the pressure was further reduced back down to zero. In the other instruments (*C*, *D*, and *E*) an up–down difference gradually became evident as the pressure was reduced back down to zero. The largest differences between initial and "final" ion currents at $10^{-7}$ Pa were shown by PPA *A* and ranged from 25% to 80% of initial value. Corresponding differences for PPA *B* ranged from 10% to 20%, and from 5% to 15% for instruments *C*, *D*, and *E*, with PPA *D* exhibiting the smallest changes. Apparent sensitivity differences at $10^{-7}$ Pa in the ion gauges were also limited to 15% or less. Since all the instruments were simultaneously exposed to the same schedule of pressure changes, the distinctly larger hysteresis exhibited by instruments *A* and *B* cannot be ascribed solely to pressure measurement errors arising from adsorption/desorption phenomena in the chamber, but rather is due to the individual hysteresis characteristics of these two instruments. One possible explanation for the hysteresis seen in these instruments is the alteration of ion energy as a result of the buildup and slow decay of surface charges.[39,40]

As in the case of linearity measurements, the attempted hysteresis measurements with less-inert gases ($H_2$, CO, $O_2$, $N_2O$, and $CO_2$) yielded results which depended much more strongly on the rate at which the test gas pressure was varied—the apparent sensitivities changed with very long (hours) time constants. Similar behavior was shown by the ion gauges. Changing the pressure at much slower rates (e.g., allowing as long as 1 h for the signals to stabilize before each measurement), resulted in smaller hysteresis effects. Some of this may be due to changes in PPA performance, but we believe that a large part of this effect was due to true slow changes in the calibration gas pressure. Using inert gases, an equilibrium pressure could be established in a matter of minutes, limited by the gas flow rate and the volume of the calibration chamber. However, during high pressure ($> 10^{-4}$

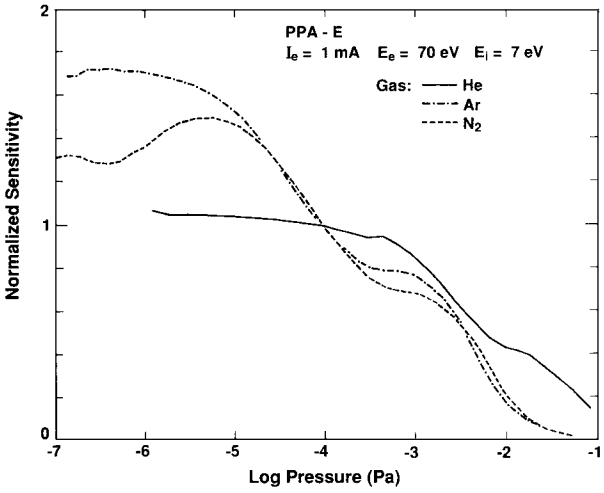


FIG. 19. Influence of gas species on linearity in one of the test instruments (PPA *E*) which showed significant nonlinearity at low pressure. Each curve is normalized to a value of 1 at $10^{-4}$ Pa. Ion source parameters set at $I_e(\text{mA})/E_e(\text{eV})/E_i(\text{eV}) = 1.45/58/6$.

Pa) $O_2$ measurements, the MDGs, which do not employ a hot filament, indicated that the pressure was approaching equilibrium with a time constant of hours. This occured even with the PPAs turned off, and we therefore believe it was caused by adsorption in the calibration chamber. We believe that this same phenomenon may account for part of the long response time observed for the PPAs at lower pressures with other active gases.

## D. Instrument–gas interactions

In general, it must be expected that the measuring instrument (the PPA) and the gas in which it operates each will, to some extent, affect properties of the other. We will use the term *interference* to refer to the influence of one gas on an instrument's sensitivity and linearity to another gas and the term *instrumental perturbation* to refer to the influence of the instrument on the pressure and composition of the gas in which it operates.

### 1. Interference

In most applications it is important to know the extent to which the composition and total pressure of a gas influences the signal developed from a particular component of the gas. Apart from the problem of overlapping neighboring peaks, there are a number of reports in the literature of such interference effects. For example, the sensitivity to helium in a He–Ar mixture has been found to change as the argon pressure was varied.[35] Similarly, in another experiment, the signal due to a constant partial pressure of krypton depended on the argon carrier gas pressure.[37] In another instance, it has been reported that ion currents developed from residual gases, believed to be at constant pressure, depended on a much larger total pressure, mainly argon.[41]

We have investigated such effects by measuring the response to a constant pressure, typically $10^{-6}$ Pa, of a trace gas as the pressure of a matrix gas was varied between $10^{-7}$ and $10^{-1}$ Pa. Curve 1 of Fig. 20 shows the results of a measurement of helium signal for PPA *E* at a constant partial pressure of helium as the presssure of the matrix gas (argon) was varied; conversely, curve 3 gives the results for a trace of argon in a variable pressure helium matrix. Shown also is the pressure dependence of the sensitivity to the matrix gas alone (curves 2 and 4). Apart from deviations at high pressure ($> 10^{-3}$ Pa), the results given in Fig. 20 show that the signal developed from the constant-pressure trace gas and the sensitivity to the matrix gas both exhibited the same dependence on the matrix gas pressure. This suggests that the mechanism responsible for the basic nonlinearity also causes the signal for one gas to depend on the pressure of another.

A similar conclusion can be drawn from the data presented in Fig. 21 for PPA *C*. The ionizer parameters chosen in this case resulted in nonlinear behavior only at high pressure. The magnitudes of the nonlinearities differed for the trace and the matrix gases, but the similarity in the pressure dependence is evident. Examination of the results obtained with the other instruments also suggests that as a general rule, at least in the case of a trace of He in Ar and vice versa, the trace gas signal depends on the matrix gas pressure in the same way that the instrument's matrix gas sensitivity depends on matrix gas pressure.

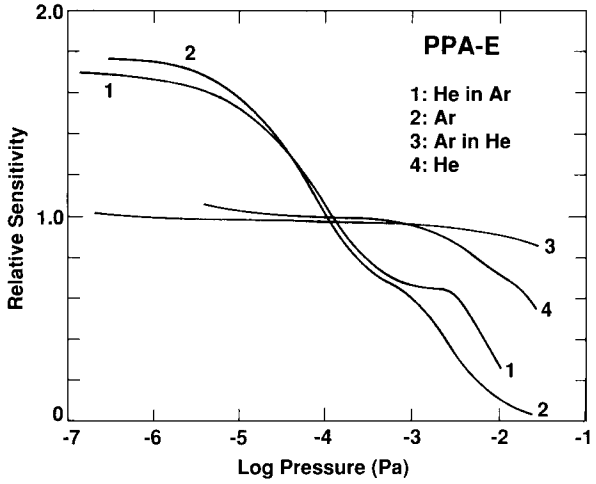


FIG. 20. Curves 1 and 3 show *ion signal* developed from a constant-pressure ($10^{-6}$ Pa) trace gas as the pressure of another gas (the matrix) is varied. Data is for PPA *E*, an instrument which exhibited significant nonlinearity at low pressures. Curves 2 and 4 show the pressure dependence of the instrument's *sensitivity* to the pure matrix gas. All curves normalized to a value near 1 at $10^{-4}$ Pa. Ion source parameters were set at $I_e$(mA)/$E_e$(eV)/$E_i$ (eV) = 1.45/58/6.

Another type of interference effect was evident when active gases were introduced. In a second set of experiments, a constant flow of an equal-parts $He/N_2/Ar$ mixture was established, creating a total pressure of about $10^{-4}$ Pa in the calibration chamber. Different test gases were then introduced at a partial pressure of about $10^{-4}$ Pa for a period of about two min. The $He^+$, $N_2^+$, and $Ar^+$ signals were continuously monitored during this process. When the test gas was relatively inert (He, Ar, $N_2$) there was no significant difference between the monitored signals before exposure and about ten min after exposure to the test gas. However,

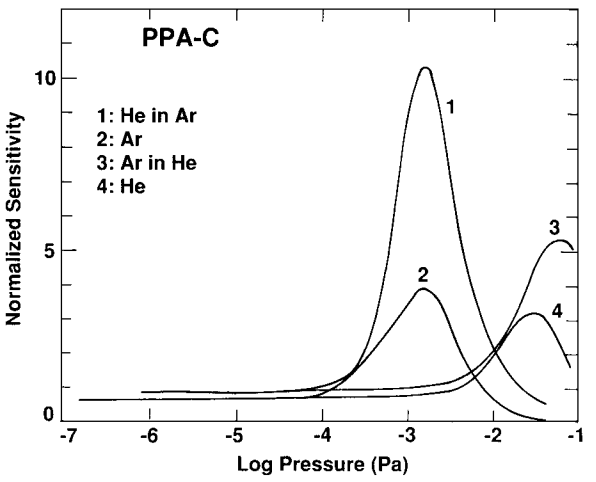


FIG. 21. Curves 1 and 3 show *ion signal* developed from a constant-pressure ($10^{-6}$ Pa) trace gas as the pressure of another gas (the matrix) is varied. Data is for PPA *C*, with ionizer parameters chosen to obtain nonlinearity at high pressures. Curves 2 and 4 show pressure dependence of the instrument's *sensitivity* to the pure matrix gas. All curves normalized to have a value near 1 at $10^{-4}$ Pa. Ion source parameters $I_e$(mA)/$E_e$(eV)/$E_i$ (eV) = 1/60/3.

immediately following the brief exposure to active test gases ($CH_4$, $H_2$, CO, $CO_2$, $C_3H_8$, and $O_2$) the $He^+$, $N_2^+$, and $Ar^+$ signals all had changed by the same factor, which ranged from 2% to 10%. Sensitivity increased in some of the instruments and decreased in others, and a slow return of sensitivities to pre-exposure values was observed. These effects are illustrated for PPAs *A*, *D*, and *E* in Fig. 22, for the case of $O_2$ test gas exposure. The largest changes occured with $O_2$ and $C_3H_8$, and for a given instrument these two gases always caused sensitivity changes in opposite directions. If higher pressure of the active test gas was used, the changes in the sensitivities for the mixture components were larger. In contrast to the PPAs, ion currents in the BA gauges very promptly returned to previous values following the brief exposure to the test gas.

We can only speculate as to the cause of this effect. Changes in filament properties would seem to be ruled out by the lack of an effect in the ion gauges. Possibly the active gases caused the generation and deposition of conducting films on insulators, or insulating films on the quadrupole rods. Subsequent operation may have reduced or oxidized these films. As mentioned in the section on hysteresis, surface charging[39,40] can cause changes in the sensitivity. In particular, changes of only a few parts per thousand in the dc potential on the rods can cause much larger changes in the ion current transmitted by the quadrupole.[26,28]

### 2. Instrumental perturbations

As with both hot and cold cathode ionization gauges, the possibility exists that a PPA will perturb the pressure to be measured. Depending on its history, a PPA can be either a source or a sink for gas. This may explain part of the long-time-constant effects which were observed with the active gases. In the present work we have not attempted to study instrumental perturbation effects in detail for the test PPAs. However, these problems are discussed in number of published works. These effects, which can cause major difficulties in the measurement of active gases, arise through electron stimulated desorption,[42–45] and chemical and electronic pumping.[45,46] There are reports in the literature of solutions to these problems for particular gases, e.g., $(CH_3)_4Pb$,[47] $SiF_4$,[48] $H_2$,[49] $H_2O$,[50] and $O_2$.[51] In many cases the interactions can be quite complicated—active gases may react to form other gaseous compounds, or they may displace previously adsorbed gases. A general solution to these problems is to "condition" the PPA and the system with a continued exposure to the gas of interest until equilibrium is established. This implies that a repeatable steady-state condition can be achieved. If this is the case, the time constants may be quite long and this conditioning process must be used during both the calibration and the measurement.

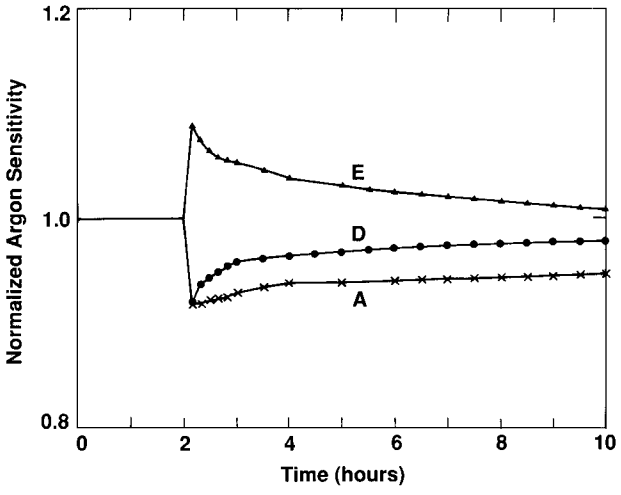


FIG. 22. Transient shift in Ar sensitivity of instruments *A*, *D*, and *E* at $P[Ar] \approx 3 \times 10^{-5}$ Pa following brief exposure (2 min) to $O_2$ at $10^{-4}$ Pa at time = 2 h. Data are normalized to have value 1 for time < 2 h. Instruments *B* and *C* also exhibited a transient shift of comparable magnitude, but for clarity, the data are not shown in this figure.

### E. Stability of sensitivity with time and use

The stability of an instrument determines how often calibration is required to assure a desired level of accuracy or, conversely, it determines the level of accuracy that can be expected as a function of time since calibration. PPA specification sheets often include a figure called "stability" but this generally refers to the electrical stability of certain supply circuits or emission regulation, rather than to the measurement characteristic of the instrument as a whole.

We have evaluated the stability of our PPAs from the repeated measurements of the absolute argon sensitivities with the operating parameters at the base settings. As noted before, Faraday cups were used for all measurements, all instruments were calibrated simultaneously, PPAs *A* and *C* had thoria-coated iridium filaments; the others were tungsten.

The stability of the absolute sensitivity can be seen in Fig. 23. These are absolute argon sensitivity measurements at $10^{-4}$ Pa, with operating parameters set to base values. The sensitivities for each instrument have been normalized by their average value over the 220 day test period. Data for the nude ion gauge are shown at the bottom of the figure. Up to day 130 the instruments were operated only with inert gases. During this time relatively large changes were observed for PPA *A*, significant changes were observed in the sensitivities of instruments *B* and *E*, while *C* and *D* were more stable. The experiments with active gases were then conducted, and argon calibrations were not performed again until day 200. As noted before, exposure to active gases caused an immediate change in sensitivity, that then decayed over a period of hours to days. The data of Fig. 23, particularly for *C* and *D*, suggest that active-gas exposure may also cause "permanent" shifts as well. The ion gauge appears to be relatively stable and unaffected.

Similar results have been reported by other authors. Ellefson presents long-term stability data for a cycloid-type spectrometer indicating a + 20% change over a 4 yr period.[52] Other authors report much higher changes in the absolute sensitivities of quadrupole instruments. Blanchard *et al.*,[53] using PPAs equipped with rhenium filaments, reported sensitivity changes as large as a factor of 2 over intervals of a few weeks, with the largest changes correlated with extended

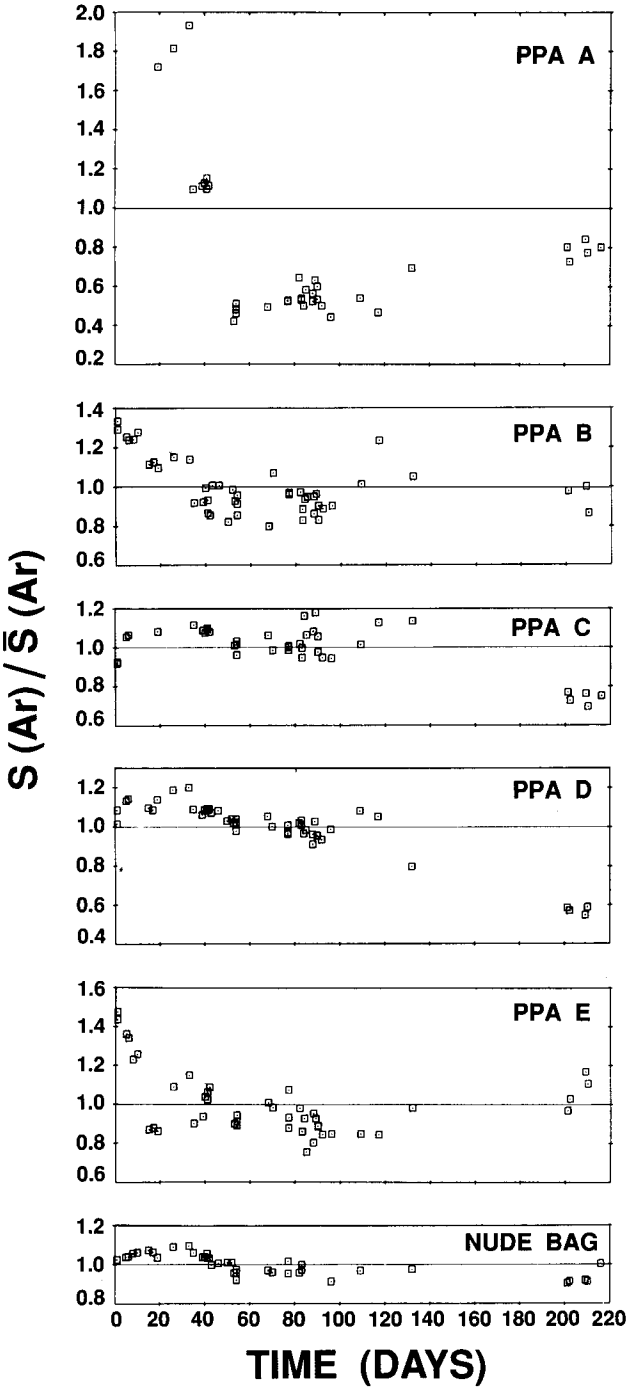


FIG. 23. Repeated Ar sensitivity measurements at the base set of operating parameters for the five test instruments over a 220-d period. In each plot, the data are normalized by $\bar{S}$[Ar], the arithmetic average of all the measurements for that instrument. For days 0–129, the instruments were exposed only to inert gases (He, $N_2$, and Ar).

exposure to $H_2$ at pressure $> 10^{-3}$ Pa. When the rhenium filaments were replaced with tungsten, week to week variations in sensitivity were found to be significantly smaller (usually $< 10\%$). Calcatelli *et al.*,[54] in a year long history of a quadrupole PPA operated with a Faraday cup, indicate sensitivity changes of up to 20% between calibrations, including a 20% increase over 50 d while the PPA was left at base pressure. The authors speculate that this might have been caused by changes in surface properties, particularly that of the ion collector. Holme *et al.*, [55] also report long-term stability data on a quadrupole, estimating $\Delta S/S$ to be invariant within $+1\%$ over a one-day period and within $+10\%$ over a one-year period. The use of electron multipliers are expected to decrease the stability even more, especially when they are new. Dylla[36] reports a decrease of instrument sensitivity by a factor of 5 after a few weeks, and attributes it to the aging of a new multiplier. Smaller long-term decrease in sensitivity, also attributed to multiplier aging, is reported in Ref. 53. In many applications (e.g., concentration measurements) only the stability of the relative sensitivities are of importance. These are generally more stable than the absolute sensitivities. Ellefson[52] reports that the ratios of sensitivities are at least one order of magnitude more stable than absolute sensitivities.

Since the linearity of the instruments has been shown to be highly dependent on operating parameters, one might also question, how stable is the linearity characteristic with time. Figure 24 includes five separate calibrations of PPA *D*, with the same operating parameters, over a 35-d period. In order to highlight any changes in the linearity, each data set has been normalized by the sensitivity at $10^{-4}$ Pa. As can be seen, the linearity is essentially unchanged over this time period. The standard deviation about the mean of the five absolute sensitivity measurements at $10^{-4}$ Pa was 3%. However, as shown in Fig. 25, over the same 35-d interval the data for PPA *A* indicated significant changes in the linearity. The absolute argon sensitivity of PPA *A* at $10^{-4}$ Pa during this same period ranged from $2.2\times10^{-6}$ A/Pa on day 1, to $1.5\times10^{-6}$ A/Pa on day 14, to $1.0\times10^{-6}$ A/Pa on days 30, 34, and 35. Results for the other instruments were intermediate between these two extremes.

## IV. CONCLUSIONS

In a long-term examination of sensitivity, resolution, linearity, interference, and stabilty we were able to obtain a

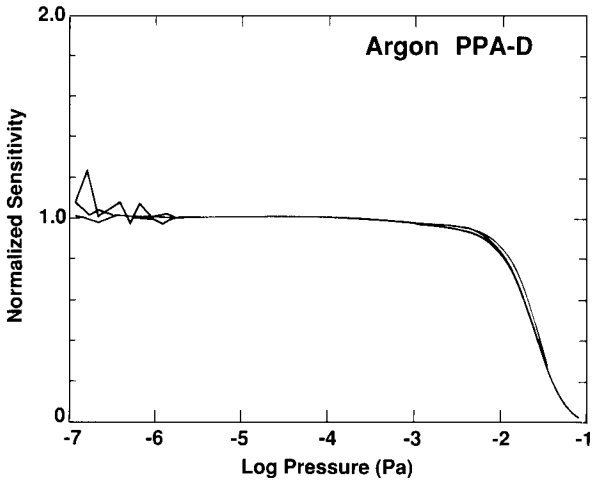


FIG. 24. Stability with time of the linearity (sensitivity vs pressure) of PPA *D* in argon over a 35-d period. Five separate curves are plotted here, each normalized to a value of 1 at $10^{-4}$ Pa. The standard deviation about the mean of the five absolute sensitivity measurements at $10^{-4}$ Pa was 3%. Ion source parameters were $I_e$(mA)/$E_e$(eV)/$E_i$(eV) = 1/60/5.

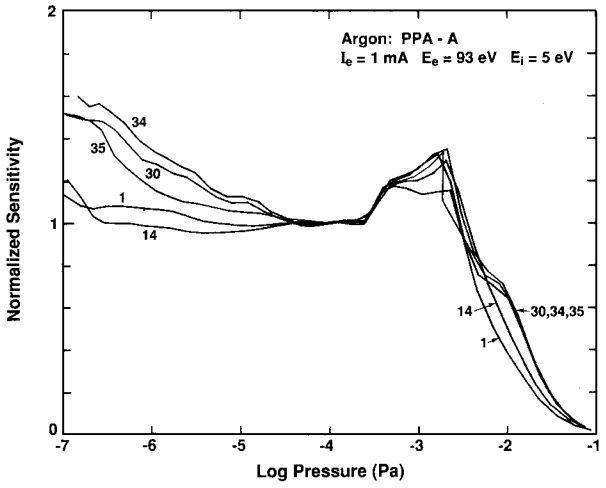


FIG. 25. Stability with time of the linearity (sensitivity vs pressure) of PPA *A* in argon over a 35-d period. Five separate curves are plotted here, each normalized to a value of 1 at $10^{-4}$ Pa. Curve labels identify specific days of the 35-d period. The absolute sensitivity measurements determined at $10^{-4}$ Pa on each of the five days ranged from $2.2\times10^{-6}$ A/Pa on day 1, to $1.5\times10^{-6}$ A/Pa on d 14, to $1.0\times10^{-6}$ A/Pa on d 30, 34, and 35. Ion source parameters were $I_e$(mA)/$E_e$(eV)/$E_i$(eV) = 1/93/5.

complete set of data for only five instruments, each of different manufacture. In many cases we do not understand the fundamental causes of the observed behavior. Therefore, we cannot say to what extent our results are typical of a particular design, let alone how typical they are of commercial PPAs in general. In addition, the importance of the various performance factors for a PPA will depend on its intended application. However, even with these limitations, these data clearly show that for many applications the performance of these PPAs differed considerably. Some of the instruments, with calibration, could attain uncertainties of a few percent. The behavior of other instruments was so complicated and dependent on operating parameters that calibration would be a difficult and even questionable task and in some cases very large errors are possible. In particular, for these worst-case instruments, the wide variation in relative sensitivities could cause errors as large as two orders of magnitude in the measurement of relative partial pressures. Similarly, the dependence of trace gas sensitivity on matrix gas pressure could cause errors of the same magnitude in determining the low-level concentrations of trace gases. The use of active gases clearly complicates the problems. A review of the data suggests that many of the undesirable characteristics may be due to space charge effects in the ionizers.

While the examples cited above are extreme, and the errors will be smaller with other instruments or operating conditions, they should cause the user to examine his or her assumptions about the behavior of PPAs and to recognize the effort required to obtain quantitative results. In order to obtain accurate partial pressure measurements it is desirable to select a well-behaved instrument and it is necessary to calibrate it. These can be difficult tasks, particularly when gas interference effects are significant. However, useful calibration results can be obtained using calibrated Bayard–Alpert ionization gauges as reference standards. In general, ion gauges are much more linear, stable, and predictable than any of the PPAs that we tested, and such a calibration will serve to determine the PPA's sensitivity and linearity with single-component gases. At high pressures ($> 10^{-4}$ Pa), better accuracy can be obtained if the ion gauge and PPA are calibrated against a molecular drag gauge. Such determination of an instrument's linearity with single-component gases may be particularly useful since the present results indicate that, when analyzing a mixture, gas interference effects will be minimal with a linear instrument. If the PPA is nonlinear, then partial pressure sensitivities will probably depend on the pressure of other gases. Periodic comparisons with the ion gauge, again with single-component gases, will serve to monitor the stability of the PPA. The accuracy of these results will be limited by the performance of both the PPA and the ion gauge, but will surely be much better than the results obtained with an uncalibrated PPA. For the accurate measurement of partial pressures one requires appropriate instrumentation and knowledge of the characteristics of that instrumentation, as well as an understanding of the measurement process.

## ACKNOWLEDGMENT

The authors wish to thank the Office of Fusion Energy of the United States Department of Energy for financial support of this work.

[1]D. Lichtman, J. Vac. Sci. Technol. A **5**, 140 (1987).
[2]D. Lichtman, J. Vac. Sci. Technol. A **2**, 200 (1984).
[3]H. W. Werner, Vacuum **33**, 521 (1983).
[4]W. K. Huber, Vacuum **13**, 399 (1964); **13**, 469 (1964).
[5]G. F. Weston, Vacuum **30**, 49 (1980).
[6]M. J. Drinkwine and D. Lichtman, *Partial Pressure Analyzers and Analysis*, edited by N. R. Whetten and R. Long, Jr., American Vacuum Society Monograph Series (American Vacuum Society, New York, 1979).
[7]P. H. Dawson, Mass Spectrom. Rev. **5**, 1 (1986).
[8]P. H. Dawson, J. Vac. Sci. Technol. A **4**, 1709 (1986).
[9]C. Greaves, Vacuum **20**, 65 (1970).
[10]J. K. Fremerey, Vacuum **32**, 685 (1982); J. Vac. Sci. Technol. A **3**, 1715 (1985).
[11]C. R. Tilford, S. Dittmann, and K. E. McCulloh, J. Vac. Sci. Technol. A **6**, 2853 (1988).
[12]R. N. Bloomer, Br. J. Appl. Phys. **8**, 83 (1957).
[13]C. F. Robinson and A. G. Sharkey, Jr., Rev. Sci. Instrum. **29**, 250 (1958).
[14]C. E. Melton, Rev. Sci. Instrum. **29**, 250 (1958).
[15]P. E. Gear, Vacuum **26**, 3 (1976).
[16]J. H. Singleton, J. Chem. Phys. **45**, 2819 (1966).
[17]B. Pödör, Vacuum **33**, 67 (1983).
[18]L. J. Kieffer and G. H. Dunn, Rev. Mod. Phys. **38**, 1 (1966).
[19]D. Mathur and C. Badrinathan, Int. J. Mass Spectrom. Ion Processes **57**, 167 (1984).
[20]T. D. Märk and A. W. Castleman, J. Phys. E **13**, 1121 (1980).
[21]P. H. Dawson, in *Quadrupole Mass Spectrometry and Its Applications*, edited by P. H. Dawson, (Elsevier, Amsterdam, 1976), p. 24.
[22]W. M. Brubaker, NASA, Report No. NASW 1298 (1970).
[23]W. E. Austin, A. E. Holme, and J. H. Leck, in Ref. 21, Fig. 6.17 p. 142.
[24]P. H. Dawson, Adv. Electron. Electron Phys. **53**, 153 (1980).
[25]P. Marchand and P. Marmet, Can. J. Phys. **42**, 1914 (1964).
[26]F. M. Mao and J. H. Leck, Vacuum **37**, 669 (1987).
[27]T. A. Flaim and P. D. Ownby, J. Vac. Sci. Technol. **8**, 661 (1971).
[28]W. G. Bley, Vacuum **38**, 103 (1988).
[29]R. D. Craig and E. H. Harden, Vacuum **16**, 67 (1966).
[30]E. D'Anna, G. Leggieri, A. Luches, and A. Perrone, J. Vac. Sci. Technol. A **5**, 3436 (1987).
[31]T. C. Ehlert, J. Phys. E **3**, 237 (1970).

[32]P. H. Dawson, Adv. Electron. Electron Phys. Suppl. **13B**, 173 (1980).
[33]R. D. Collins, Vacuum **19**, 105 (1969).
[34]N. R. Reagan, L. C. Frees, and J. W. Gray, J. Vac. Sci. Technol. A **5**, 2389 (1987).
[35]W. E. Austin, F. M. Mao, J. M. Yang, and J. H. Leck, J. Vac. Sci. Technol. A **5**, 2631 (1987).
[36]H. F. Dylla, in Proceedings of the Ninth International Vacuum Congress and Fifth International Conference on Solid Surfaces, edited by J. L. deSegovia, Madrid, 1983 (unpublished), Fig. 6, p. 578.
[37]F. M. Mao, J. M. Yang, W. E. Austin, and J. H. Leck, Vacuum **37**, 335 (1987).
[38]R. J. Reid and A. P. James, Vacuum **37**, 339 (1987).
[39]P. Marmet, P. Marchand, and C. Paquet, in *Proceedings of the International Conference on Mass Spectroscopy, Kyoto, 1969,* edited by K. Ogata and T. Hayakawa (University of Tokyo, Tokyo, 1970) p. 765.
[40]Y. Petit-Clerk and J. D. Carette, Vacuum **18**, 7 (1968).
[41]P. L. Swart and H. Aharoni, J. Vac. Sci. Technol. A **3**, 1935 (1985).
[42]T. E. Madey and J. T. Yates, Jr., J. Vac. Sci. Technol. **8**, 525 (1971).
[43]A. Breth, R. Dobrozemsky, and B. Kraus, Vacuum **33**, 73 (1983).
[44]P. A. Redhead, J. Vac. Sci. Technol. **7**, 182 (1970).
[45]P. A. Redhead, J. P. Hobson, and E. V. Kornelsen, *The Physical Basis of Ultrahigh Vacuum* (Chapman and Hall, London, 1968).
[46]R. D. Willis, S. L. Allman, C. H. Chen, G. D. Alton, and G. S. Hurst, J. Vac. Sci. Technol. A **2**, 57 (1984).
[47]J. H. Batey, Int. J. Mass Spectrom. Ion Processes **60**, 117 (1984).
[48]E. Hasler and G. Rettinghaus, Vacuum **38**, 777 (1988).
[49]H. F. Dylla and W. R. Blanchard, J. Vac. Sci. Technol. A **1**, 1297 (1983).
[50]L. C. Frees, D. H. Holkeboer, and J. Farden, in Proceedings of the 30th Annual Conference on Mass Spectrometry, Honolulu, 1982 (unpublished), p. 656.
[51]L. Lieszkovszky and J. Borossay, J. Vac. Sci. Technol. A **5**, 2819 (1987).
[52]R. E. Ellefson, D. Cain, and C. N. Lindsay, J. Vac. Sci. Technol. A **5**, 134 (1987).
[53]W. R. Blanchard, P. J. McCarthy, H. F. Dylla, P. H. LaMarche, and J. E. Simpkins, J. Vac. Sci. Technol. A **4**, 1715 (1986).
[54]A. Calcatelli, M. Bergoglio, and G. Rumiano, J. Vac. Sci. Technol. A **5**, 2464 (1987).
[55]A. E. Holme, W. J. Thatcher, and J. H. Leck, Vacuum **24**, 7 (1974).